

## Low Phase Noise RF Oscillators Based on Thin-Film Lithium Niobate Acoustic Delay Lines

Li, Ming Huang; Lu, Ruochen; Manzaneque, Tomas; Gong, Songbin

**DOI**

[10.1109/JMEMS.2019.2961976](https://doi.org/10.1109/JMEMS.2019.2961976)

**Publication date**

2020

**Document Version**

Final published version

**Published in**

Journal of Microelectromechanical Systems

**Citation (APA)**

Li, M. H., Lu, R., Manzaneque, T., & Gong, S. (2020). Low Phase Noise RF Oscillators Based on Thin-Film Lithium Niobate Acoustic Delay Lines. *Journal of Microelectromechanical Systems*, 29(2), 129-131. <https://doi.org/10.1109/JMEMS.2019.2961976>

**Important note**

To cite this publication, please use the final published version (if applicable). Please check the document version above.

**Copyright**

Other than for strictly personal use, it is not permitted to download, forward or distribute the text or part of it, without the consent of the author(s) and/or copyright holder(s), unless the work is under an open content license such as Creative Commons.

**Takedown policy**

Please contact us and provide details if you believe this document breaches copyrights. We will remove access to the work immediately and investigate your claim.

# Low Phase Noise RF Oscillators Based on Thin-Film Lithium Niobate Acoustic Delay Lines

Ming-Huang Li<sup>1b</sup>, Member, IEEE, Ruochen Lu<sup>1b</sup>, Member, IEEE, Tomás Manzaneque<sup>1b</sup>, Member, IEEE, and Songbin Gong<sup>1b</sup>, Senior Member, IEEE

**Abstract**—An RF oscillator has been demonstrated using a wideband SH<sub>0</sub> mode lithium niobate acoustic delay line (ADL). The design space of the ADL-based oscillators is theoretically investigated using the classical linear time-invariant (LTI) phase noise model. The analysis reveals that the key to low phase noise is low insertion loss (IL), large delay ( $\tau_G$ ), and high carrier frequency ( $f_o$ ). Two SH<sub>0</sub> ADL oscillators based on a single SH<sub>0</sub> ADL ( $f_o = 157\text{MHz}$ , IL = 3.2 dB,  $\tau_G = 270$  ns) but with different loop amplifiers have been measured, showing low phase noise of  $-114$  dBc/Hz and  $-127$  dBc/Hz at 10-kHz offset with a carrier power level of  $-8$  dBm and 0.5 dBm, respectively. These oscillators not only have surpassed other Lamb wave delay oscillators but also compete favorably with surface acoustic wave (SAW) delay line oscillators in performance. [2019-0223]

**Index Terms**—Microelectromechanical systems, lithium niobate, acoustic delay lines, oscillator, piezoelectric transducers, phase noise.

## I. INTRODUCTION

ACOUSTIC delay lines (ADL) are a versatile building block for a wide range of applications, including filters [1], environmental sensors [2], nonreciprocal components [3], and RF frequency references [4], [5]. They are conventionally built with surface acoustic wave (SAW) technology. As a promising alternative, recent efforts have been devoted to developing high-performance plate wave ADLs based on lithium niobate (LiNbO<sub>3</sub>) thin films [6]–[8]. In contrast to SAW ADLs, LiNbO<sub>3</sub> plate wave ADLs show higher electro-mechanical coupling ( $k^2$ ) and better reflectivity ( $\Gamma$ ) per wavelength, which lead to significantly lower IL, wider FBW, and better center frequency ( $f_o$ ) scalability over a wide range of time delay ( $\tau_G$ ) [9]. Such improvement can be especially beneficial to the RF oscillator design based on ADLs for either a single-mode oscillator [10] or comb frequency generator [11]. Low IL, long delay, and high  $f_o$  are the key to low phase noise (PN) and DC-power reduction, while wide FBW can be leveraged for frequency tuning.

To exploit the advances made in LiNbO<sub>3</sub> plate wave ADLs, we seek to demonstrate the first oscillator based on this newly

emerged delay line technology in this work. A previous developed fundamental shear horizontal (SH<sub>0</sub>) mode VHF ADL with  $f_o = 157$  MHz, IL = 3.2 dB,  $\tau_G = 270$  ns, and FBW > 6% is used as the frequency selecting element [6]. Two commercially-off-the-shelf (COTS) low noise amplifiers, namely MAR-6+ and ZFL-1000LN+, are used to configure two distinct oscillator circuits with different carrier power. Finally, the oscillator performance is evaluated based on phase noise and dc-current consumption. Proposed LiNbO<sub>3</sub> ADL oscillators show significantly better performance than the Lamb wave ADL oscillator in literature [10], while also attaining performance comparable to commercial SAW ADL oscillators but at lower carrier power [12], [13].

Manuscript received October 3, 2019; revised December 5, 2019; accepted December 19, 2019. Date of publication January 9, 2020; date of current version April 2, 2020. This work was supported in part by the DARPA NZero Program, in part by the NSF SpecEES Program under Grant 1824320, and in part by the Ministry of Science and Technology (MOST) of Taiwan under Grant MOST 108-2636-E-007-014 (Young Scholar Fellowship Program). Subject Editor C. Nguyen. (Corresponding author: Ming-Huang Li.)

Ming-Huang Li is with the Department of Power Mechanical Engineering, National Tsing Hua University, Hsinchu 30013, Taiwan (e-mail: mhli@pme.nthu.edu.tw).

Ruochen Lu and Songbin Gong are with the Department of Electrical and Computer Engineering, University of Illinois at Urbana-Champaign, Urbana, IL 61801 USA (e-mail: rlu10@illinois.edu; songbin@illinois.edu).

Tomás Manzaneque is with the Department of Precision and Microsystems Engineering, Delft University of Technology, 2628 CD Delft, The Netherlands (e-mail: t.manzanequeGarcia@tudelft.nl).

Color versions of one or more of the figures in this article are available online at <http://ieeexplore.ieee.org>.

Digital Object Identifier 10.1109/JMEMS.2019.2961976

1057-7157 © 2020 IEEE. Personal use is permitted, but republication/redistribution requires IEEE permission.

See <https://www.ieee.org/publications/rights/index.html> for more information.

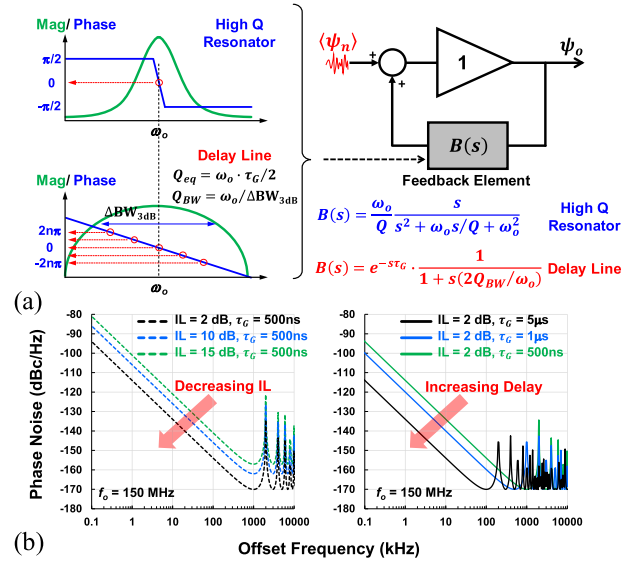


Fig. 1. (a) Schematic of the LTI phase-space model for general oscillators employed a high- $Q$  resonator or a delay line as the frequency selection element. (b) Simulated phase noise for a 150 MHz delay line oscillator with respect to IL and delay. Assumed a wideband delay line with  $Q_{BW} = 5$ .

emerged delay line technology in this work. A previous developed fundamental shear horizontal (SH<sub>0</sub>) mode VHF ADL with  $f_o = 157$  MHz, IL = 3.2 dB,  $\tau_G = 270$  ns, and FBW > 6% is used as the frequency selecting element [6]. Two commercially-off-the-shelf (COTS) low noise amplifiers, namely MAR-6+ and ZFL-1000LN+, are used to configure two distinct oscillator circuits with different carrier power. Finally, the oscillator performance is evaluated based on phase noise and dc-current consumption. Proposed LiNbO<sub>3</sub> ADL oscillators show significantly better performance than the Lamb wave ADL oscillator in literature [10], while also attaining performance comparable to commercial SAW ADL oscillators but at lower carrier power [12], [13].

## II. ADL BASED OSCILLATOR

### A. Phase Noise for ADL-Based Oscillator

Fig. 1(a) depicts a general phase-space model of a feedback oscillator where the feedback element can be a high- $Q$  resonator or a delay line (DL). Unlike the high- $Q$  resonator, a DL oscillator can operate at different modes within its bandwidth [9]. The spacing of adjacent modes is determined by the reciprocal delay time of the DL, which is given by

$$\tau_G = \frac{d\phi}{d\omega} = \frac{2Q_{eq}}{\omega_o} \quad (1)$$

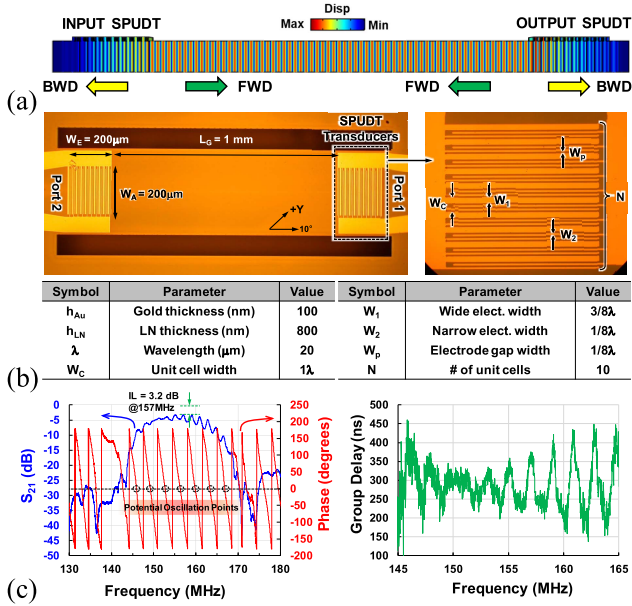


Fig. 2. (a) Cross-sectional mode shape of the SH<sub>0</sub> ADL with 10 SPUDT cells. The thickness of the cross-section is exaggerated. (b) Optical microscope images and key parameters of the fabricated ADL. (c) Open-loop measurement result of the SH<sub>0</sub> ADL with matching networks.

where  $Q_{eq}$  is the equivalent quality factor of the delay line. Therefore, a DL with large  $\tau_G$  and high  $\omega_o$  can be viewed as a high- $Q$  element. The single-side band (SSB) bandpass response of the ADL can be modeled as a delay element with a selection filter in phase-space, given by

$$B(s) = e^{-s\tau_G} \cdot \frac{1}{1 + s\tau_B}, \quad (2)$$

where  $s = j\Delta\omega$  is the offset frequency from the carrier in rad/s,  $\tau_B = 2Q_{BW}/\omega_o$  is the time constant of the filter [9] and  $Q_{BW}$  is derived from the 3 dB bandwidth of the ADL [Fig. 1(a)]. Once the Barkhausen criterion is satisfied, the overall phase noise spectrum can then be derived by conventional linear time-invariant (LTI) analysis as,

$$L(\Delta\omega) \approx S_{PN} \cdot |H(j\Delta\omega)|^2 \cdot \left(1 + \frac{\omega_c}{\Delta\omega}\right) \quad (3)$$

and

$$S_{PN} = 10^{(-174 - P_c + IL + NF)/10} \quad (4)$$

$$H(j\Delta\omega) = \frac{1}{1 - B(s)} \Big|_{s \rightarrow j\Delta\omega} \quad (5)$$

where  $P_c$  is the carrier power in the loop in dBm, IL is the insertion loss of the ADL in dB, NF is the noise figure of the amplifier in dB, and  $\omega_c$  is the corner frequency of  $1/f^3$  phase noise in rad/s. It is apparent that *low IL* and *large delay* are the keys to obtain low phase noise. Fig. 1(b) shows the predicted phase noise of a 150 MHz ADL oscillator using (3) while assuming  $P_c = 0$  dBm and an NF of 3 dB under various IL and delay conditions. Finally, the effective time delay in the oscillation loop is contributed by both  $\tau_G$  and  $\tau_B$  although the effect of  $\tau_B$  is not significant in comparison with  $\tau_G$ .

### B. Design of ADL

Fig. 2(a) shows the 3D displacement plot of the ADL based on 3D finite element analysis in COMSOL. In this work, the ADL consist of an X-cut 800-nm suspended LiNbO<sub>3</sub> thin film and a 100-nm Au electrode to excite the SH<sub>0</sub> wave. The elastic wave propagation

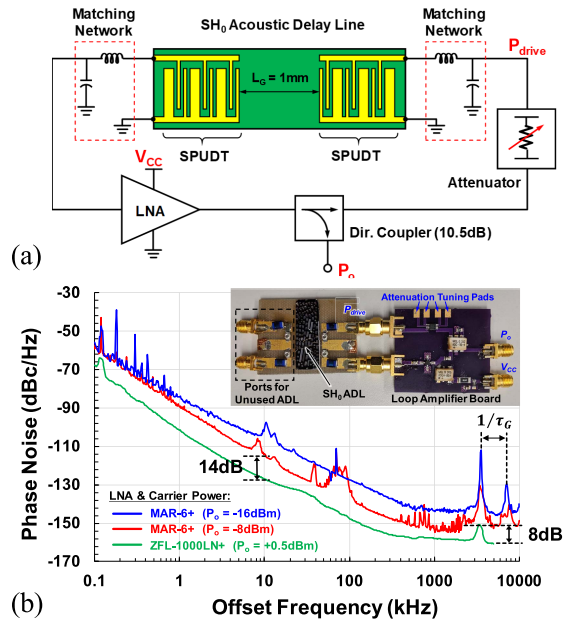


Fig. 3. (a) Circuit schematic of the ADL oscillator. (b) Measured phase noise spectrum under various carrier power levels. Inset: Oscillator board photo with MAR-6+ as the LNA.

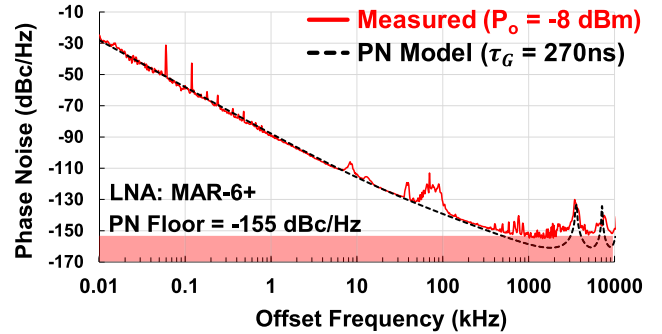


Fig. 4. Phase noise fitting for the ADL oscillator with  $\tau_G = 270$  ns and  $f_c = 15$  kHz.

direction is selected at  $-10^\circ$  to the +Y crystallographic axis for maximizing the  $k^2$ . As shown in Fig. 2(a), two sets of single-phase unidirectional transducers (SPUDT) are used to excite and receive the acoustic wave signal with minimal loss, where the detailed design procedure for SPUDT can be found in [6]. The central delay length is selected as  $L_G = 1$  mm to yield a moderate  $\tau_G = 275$  ns.

The optical images and the measured frequency spectra of the fabricated ADL are given in Fig. 2(b) and (c), respectively. The ADL is matched to 50  $\Omega$  ports using LC matching networks on the printed circuit board, showing a minimum IL of 3.2 dB at 157 MHz. We also observe that there are 7 potential oscillation points within ADL passband. With proper amplifier circuit design to meet Barkhausen condition at more than one frequency, multimode oscillation can be potentially sustained simultaneously [9]. The extracted group delay in Fig. 2(c) shows some ripples spanning from 200 to 400 ns, yielding an averaged  $\tau_G$  around 275 ns. The in-band ripples in IL and  $\tau_G$  are caused by the finite unidirectionality of the transducers used in these delay lines and internal multi-reflections [8].

## III. EXPERIMENTAL RESULTS AND DISCUSSIONS

### A. Oscillator Circuits

Fig. 3(a) shows the schematic of the oscillator circuit, which is composed of an SH<sub>0</sub> ADL, two impedance matching networks, a low

TABLE I  
COMPARISON OF ADL-BASED RF OSCILLATORS

References	[10]	[12]	[13]	This work	
Material	GaN	GaN on Si	Quartz	LiNbO <sub>3</sub>	
Device Type	Delay Line Narrow Band	Delay Line Narrow Band	Delay Line Narrow Band	Delay Line Wide Band	
Acoustic Mode	A <sub>0</sub> Lamb	SAW	SAW	SH <sub>0</sub>	
Frequency (MHz)	59.7	252	622	157	
DL Bandwidth (MHz)	–	~0.252* (0.1%)	1.3 (0.2%)	10 (6.45%)	
Insertion Loss (dB)	30.2	28.2	10	3.2	
Delay Time (ns)	–	–	–	270	
Power Supply Current, I <sub>CC</sub> (mA)	40*	40*	65	16 (MAR-6+)	48 (ZFL-1000LN+)
Max. Output Power, P <sub>omax</sub> (dBm)	15.1	5.2	13	-8**	0.5**
PN @1kHz (dBc/Hz)	-80	–	-109	-90	-101
PN @10kHz (dBc/Hz)	-120	–	-132	-114	-127
PN @300kHz (dBc/Hz)	-135	-105	-160	-148	-156

\* Extracted from the Q-factor \* The custom GaN amplifier used in [10] and [12] are the same  
\*\* Including the coupling loss of ~10 dB from the directional coupler

noise amplifier (LNA), a variable attenuator, and a directional coupler. Although several ADLs are designed on a single chip, in this work, a specific ADL is paired with two low noise amplifiers, namely MAR-6+ and ZFL-1000LN+ from Mini-Circuits, Inc., to evaluate the phase noise performance. They have with similar NF below 2.9 dB. The MAR-6+ is biased at  $V_{CC} = 6$  V for lower carrier power operation, while ZFL-1000LN+ is operated at  $V_{CC} = 15$  V to obtain larger carrier power. The variable attenuator is placed before ADL as a passive limiter to manually control the actuation power  $P_{drive}$ .

### B. Experimental Results

Fig. 3(b) shows the measured phase noise spectrum of the ADL oscillators, with the picture of the evaluation board also provided in the inset. By changing the attenuation, three phase noise curves with different carrier power are recorded. The phase noise of  $-100$  dBc/Hz,  $-114$  dBc/Hz, and  $-127$  dBc/Hz at the 10-kHz offset is measured under  $P_o = -16$ ,  $-8$ , and  $+0.5$  dBm, respectively. The slope of these phase noise curves is  $-30$  dB/decade, which may be caused by the  $1/f$  noise from the piezoelectric material [14] as well as the amplifiers [15]. Using (3), the fitted phase spectrum is presented in Fig. 4 where  $f_c = \omega_c/2\pi = 15$  kHz and  $\tau_G = 270$  ns are used to produce the best-fit. We also noticed that the phase noise slope below 10-kHz becomes steeper as the output power increases from  $-16$  dBm to  $-8$  dBm. This effect is likely caused by the thermal nonlinearity of the delay line. On the other hand, higher carrier power leads to better phase noise at far-from-carrier offsets as expected, showing a minimum phase noise floor lower than  $-161$  dBc/Hz.

Finally, we compare our work with published SAW ADL oscillators [12], [13] and Lamb wave ADL oscillators [10]. Thanks to the low IL in thin-film LiNbO<sub>3</sub> ADL, this work shows comparable phase noise performance to state-of-the-art ADL oscillators with preferable lower current consumption.

## IV. CONCLUSION

This work presents the design and characterization of the first RF oscillators enabled by thin-film LiNbO<sub>3</sub> ADLs. The oscillators show phase noise of  $-114$  dB/Hz at 10-kHz and  $-155$  dBc/Hz at 1-MHz offset at a carrier frequency of 157 MHz. The measured performance is comparable to published SAW and Lamb wave ADL oscillators but with a 16 mA drive current. The LiNbO<sub>3</sub> ADL oscillators can be further improved by using longer delays and scaling up the oscillation frequency [16].

## REFERENCES

- [1] R. H. Tancrell and M. G. Holland, "Acoustic surface wave filters," *Proc. IEEE*, vol. 59, no. 3, pp. 393–409, Mar. 1971.
- [2] A. Pohl, "A review of wireless SAW sensors," *IEEE Trans. Ultrason., Ferroelectr., Freq. Control*, vol. 47, no. 2, pp. 317–332, Mar. 2000.
- [3] R. Lu, T. Manzanque, Y. Yang, L. Gao, A. Gao, and S. Gong, "A radio frequency nonreciprocal network based on switched acoustic delay lines," *IEEE Trans. Microw. Theory Techn.*, vol. 67, no. 4, pp. 1516–1530, Apr. 2019.
- [4] L. Eichinger, F. Sischka, G. Olbrich, and R. Weigel, "Accurate design of low-noise microwave SAW oscillators," in *Proc. IEEE Ultrason. Int. Symp.*, Oct. 2000, pp. 29–34.
- [5] M.-H. Li, R. Lu, T. Manzanque, and S. Gong, "Thin-film lithium niobate acoustic delay line oscillators," in *Proc. IEEE Int. Conf. Micro Electro Mech. Syst. (MEMS)*, Jan. 2020.
- [6] T. Manzanque, R. Lu, Y. Yang, and S. Gong, "Low-loss and wideband acoustic delay lines," *IEEE Trans. Microw. Theory Techn.*, vol. 67, no. 4, pp. 1379–1391, Apr. 2019.
- [7] R. Lu, T. Manzanque, Y. Yang, M.-H. Li, and S. Gong, "GHz low-loss and wide-band S0 mode lithium niobate acoustic delay lines," *IEEE Trans. Ultrason., Ferroelectr., Freq. Control*, vol. 66, no. 8, pp. 1373–1386, Aug. 2019.
- [8] R. Lu, Y. Yang, M.-H. Li, T. Manzanque, and S. Gong, "GHz broadband SH0 mode lithium niobate acoustic delay lines," *IEEE Trans. Ultrason., Ferroelectr., Freq. Control*, to be published.
- [9] E. Rubiola, *Phase Noise and Frequency Stability in Oscillators*. Cambridge, U.K.: Cambridge Univ. Press, 2008.
- [10] X. Lu, J. Ma, C. P. Yue, and K. M. Lau, "A GaN-based Lamb-wave oscillator on silicon for high-temperature integrated sensors," *IEEE Microw. Wireless Compon. Lett.*, vol. 23, no. 6, pp. 318–320, Jun. 2013.
- [11] I. Avramov and Z. Georgiev, "A surface-acoustic-wave comb spectrum oscillator for sensor applications," *IEEE Trans. Ultrason., Ferroelectr., Freq. Control*, vol. 38, no. 4, pp. 334–336, Jul. 1991.
- [12] X. Lu, J. Ma, X. L. Zhu, C. M. Lee, C. P. Yue, and K. M. Lau, "A novel GaN-based monolithic SAW/HEMT oscillator on silicon," in *Proc. IEEE Ultrason. Int. Symp.*, Oct. 2012, pp. 2206–2209.
- [13] Integrated Device Technology, Inc. *IDT White Paper: Voltage Controlled SAW Oscillator (VCISO) Fundamentals*. Accessed: Apr. 29, 2011. [Online]. Available: <https://www.idt.com/document/whp/voltagecontrolledsawosc-vciso-fundamentals>
- [14] S. Ghosh, "Study on the origin of  $1/f$  in bulk acoustic wave resonators," Ph.D. dissertation, Univ. Franche-Comté, Besançon, France, Mar. 2015.
- [15] R. Boudot and E. Rubiola, "Phase noise in RF and microwave amplifiers," *IEEE Trans. Ultrason., Ferroelectr., Freq. Control*, vol. 59, no. 12, pp. 2613–2624, Dec. 2012.
- [16] R. Lu, T. Manzanque, Y. Yang, M.-H. Li, and S. Gong, "Towards digitally addressable delay synthesis: GHz low-loss acoustic delay elements from 20 NS to 900 NS," in *Proc. IEEE Int. Conf. Micro Electro Mech. Syst. (MEMS)*, Jan. 2019, pp. 121–124.